J Appl Electrochem (2007) 37:905–912
DOI 10.1007/s10800-007-9329-x

ORIGINAL PAPER

Roles of adsorbed OH and adsorbed H in the oxidation of hydrogen and the reduction of UO_2^{2+} ions at Pt electrodes under non-conventional conditions

Jei-Won Yeon · Su-Il Pyun

Received: 30 September 2006 / Accepted: 26 March 2007 / Published online: 17 April 2007

Abstract The roles of adsorbed hydroxyl radicals, OH, at a high temperature and adsorbed hydrogen atoms, H, in an acidic solution were investigated in the electrochemical reactions on Pt electrode by using potentiodynamic polarisation experiment, cyclic voltammetry and constant-potential electrolysis combined with UV/VIS analysis. From the analysis of the polarisation curves obtained from Pt electrode in a 0.185 M H_3BO_3 solution at 473 K, it was found that the reducing capability of dissolved hydrogen is significantly enhanced due to the increases of the mass transfer and the electron transfer rates. Especially, it is suggested that the stable Pt-OH_{ad} plays a significant role in the passivation reaction in the potential range from 0.60 to 0.75 V_{SHE}. From the analyses of the experimental results for the electrochemical reduction of UO_2^{2+} ions on Pt surface in a 1.0 M $HClO_4$ solution, it is recognised that the reduction reaction of UO_2^{2+} to U^{4+} ions is strongly dependent on the hydrogen atoms adsorbed on Pt electrode (indirect reduction of UO_2^{2+}) as well as on the electrons transferred from Pt electrode (direct reduction of UO_2^{2+}). In addition, the reduction mechanism of UO_2^{2+} ions involved in Pt-H_{ad} is also proposed.

J.-W. Yeon
Nuclear Chemistry Research Division, Korea Atomic Energy Research Institute, P.O. Box 105, Yuseong-gu, Daejeon 305-353, Republic of Korea

S.-I. Pyun (✉)
Department of Materials Science and Engineering, Korea Advanced Institute of Science and Technology, 373-1, Guseong-dong, Yuseong-gu, Daejeon 305-701, Republic of Korea
e-mail: sipyun@webmail.kaist.ac.kr

Keywords Adsorbed hydrogen · Adsorbed hydroxyl · Passivation · Pt electrode · Reduction of UO_2^{2+}

1 Introduction

Hydrogen gas is one of the most important chemical additives in the primary coolant of PWRs (pressurised water reactors). It is known [1, 2] that dissolved hydrogen protects the structural materials from the oxidising species produced by water radiolysis, and at the same time, hydrogen gas dissolves the CRUD (Chalk River unidentified deposits) at the end of a cycle in PWRs. Furthermore, since dissolved hydrogen may contribute to the cracking of zircaloy claddings [3–5], the corrosion of steam generator tubes [6, 7] and the deposition of CRUD [8, 9], it is necessary to understand the electrochemical oxidation behaviour of dissolved hydrogen at a high temperature. However, although it was recently found that dissolved hydrogen affects the PWR coolant system in many ways under high-duty conditions, few studies have been carried out on this reaction at a high temperature.

On the other hand, it has been well known [10] that the actinide species including uranium ions have various chemical properties according to their oxidation states in aqueous solutions. The study of the electrochemical behaviour of uranyl ions UO_2^{2+}, which are the principal corrosion product of nuclear fuels, provides an effective means to evaluate the variable chemical properties of actinide compounds. To evaluate the electrochemical reactions of chemical species including UO_2^{2+} ions, one often uses an electrochemical system coupled with other analysis tools such as an ATR-SEIRA (attenuated total reflectance-surface enhanced infrared absorption) spectrometer, an EQCM (electrochemical quartz crystal

microbalance) and a UV/VIS (ultraviolet and visible) spectrometer [11–13]. In order to apply these tools to the electrochemical system under consideration, it is necessary to employ solid noble metals such as platinum for the configuration of an appropriate electrode system. However, most studies [14–19] on the electrochemical reduction of UO_2^{2+} ions in acidic solutions have been carried out with Hg electrode to avoid the formation and evolution of hydrogen gas.

It is noted that the oxidation of dissolved hydrogen and the reduction of UO_2^{2+} ions, which have been given much attention in nuclear chemistry, are closely related to the adsorption phenomena on Pt surface. In order to acquire reliable results with Pt electrode for the oxidation of dissolved hydrogen at a high temperature and the reduction of UO_2^{2+} ions in an acidic solution, one has to understand the principal electrochemical reactions on Pt surface such as HOR (hydrogen oxidation reaction), OER (oxygen evolution reaction) and HER (hydrogen evolution reaction) [20–26]. The HOR sequence on Pt surface is assumed to proceed in the following three steps: (1) the diffusion of dissolved hydrogen from the bulk solution onto Pt surface; (2) the adsorption of the surface hydrogen atoms onto the adsorption sites on Pt; and (3) the electrochemical oxidation of adsorbed hydrogen atoms to produce hydronium ions (H_3O^+).

$$H_2(\text{dissolved}) \rightarrow H_2(\text{surface}) \quad (1)$$

$$H_2(\text{surface}) + 2\ \text{Pt} \rightarrow 2\ \text{Pt-H}_{ad} \quad (2)$$

$$\text{Pt-H}_{ad} + H_2O \rightarrow \text{Pt} + H_3O^+ + e \quad (3)$$

At a low overpotential, the electron transfer (step 3) is the dominant rate-determining step, whereas at high potentials the mass transfer (step 1) determines the total reaction rate. As the overpotential increases, Pt oxides are formed at steps 4 and 5, which are the initial stages of the OER.

$$\text{Pt} + H_2O \rightarrow \text{Pt-OH}_{ad} + H^+ + e \quad (4)$$

$$\text{Pt-OH}_{ad} \rightarrow \text{Pt-O} + H^+ + e \quad (5)$$

As the coverage of chemisorbed oxygen increases, the hydrogen oxidation current becomes smaller because of the decrease in the number of adsorption sites for hydrogen atoms, and then the oxidation of hydrogen is blockaded, followed by passivation on Pt surface [27]. The HER follows the reverse sequence of the HOR. It is generally known [20, 22, 25, 26] that the fast discharge-slow recombination mechanism has been accepted for the HER on Pt surface. Thus the recombination ($2\text{Pt-H}_{ad} \rightarrow 2\text{Pt} + H_2$) is the rate-determining step in the HER, and hydrogen atoms are considered to stably adsorb on Pt surface.

In the present work, the electrochemical behaviour of dissolved hydrogen on Pt surface was investigated in order to evaluate the reducing capability of dissolved hydrogen at a high temperature. In addition, the electrochemical reduction of UO_2^{2+} ions was examined on Pt electrode to reveal the reduction characteristics of uranium-containing species. From the experimentally measured results, two remarkable phenomena were observed: one is passivation of Pt surface at a high temperature and the other is decrease of the concentration of the reduced U^{4+} ions within a certain potential range with decreasing applied potential. These two phenomena are discussed in terms of the respective roles of Pt-OH_{ad} and Pt-H_{ad} in these two reactions.

2 Experimental

2.1 The electrochemical system for a high temperature condition

An electrochemical measurement system was designed to evaluate the oxidation behaviour of dissolved hydrogen at a high temperature. The system for measuring the polarisation curves was composed of a high-temperature electrochemical cell, a potentiostat and an electric heater. The electrochemical cell as shown in Fig. 1 was a specially manufactured titanium autoclave (PARR, USA) that had five ports for fitting the conventional 3-electrode system and a purging gas inlet/outlet. To remove any undesirable current flow during the experiments, a Teflon cup was placed in the autoclave as an insulating barrier. The potentiostat (EG&G PARC, Versastat, USA) was controlled by a personal computer (IBM 286) equipped with application software (PARC M270). And the electric heater was automatically controlled by a programmed microprocessor to maintain the solution temperature in the autoclave at a desired level.

In the electrochemical cell system, a working electrode was made with a polycrystalline Pt rod of 2 mm in diameter, which was sealed by a glass melting method except for the bottom face. The area of the working electrode being exposed to the electrolyte amounted to 0.03 cm^2. A long Pt wire of 1 mm in diameter and an Ag/AgCl electrode were used as a counter electrode and an external reference electrode, respectively.

The measured potentials in the high temperature experiments were converted against the standard hydrogen electrode (SHE) after calibrating the temperature and KCl concentration in the reference electrode [28]. Before the cell temperature increased, the inner space of the

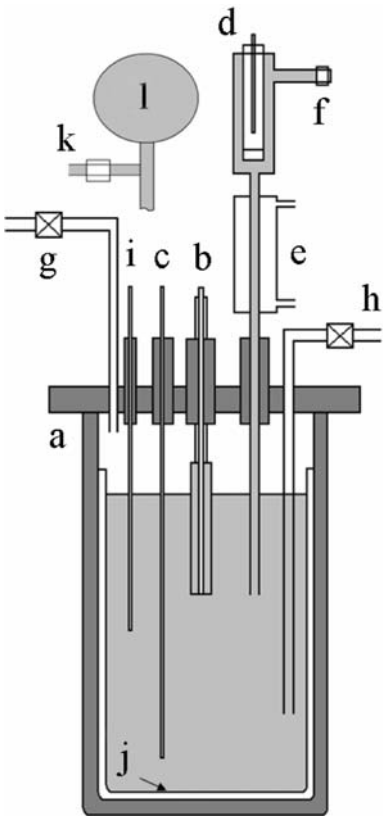

Fig. 1 Scheme of the high-temperature electrochemical measurement system: a, Ti pressure vessel; b, Pt working electrode; c, count electrode; d, external Ag/AgCl reference electrode; e, cooling water jacket; f, solution outlet; g, gas outlet; h, purge gas inlet; i, thermocouple; j, teflon cup; k, safety valve; l, steam pressure gauge

electrochemical cell was purged by high purity (99.999%) H_2 and Ar gas for more than 4 h in order to maintain the cell at hydrogenated and inert conditions, respectively. The pressure in the autoclave under inert conditions was determined by the saturated steam pressures 1 and 16 bar of the solution temperatures of 298 K and 473 K, respectively. The autoclave pressure under hydrogenated conditions was controlled to be 1 and 28 bar at 298 K and 473 K, respectively.

In order to investigate the oxidation behaviour of dissolved hydrogen at a high temperature, the potentiodynamic polarisation measurements were conducted on Pt electrode at 473 K in a 0.185 M boric acid solution at a scan rate of 5 mV s^{-1}.

2.2 The electrolysis and UV/VIS spectroscopic systems for the reduction of UO_2^{2+} ions

Electrochemical and UV/VIS spectroscopic methods were used to investigate the reduction reaction of UO_2^{2+} ions on Pt surface in acidic solution. An electrolysis cell as shown in Fig. 2 was used for the analysis of UO_2^{2+} reduction. The

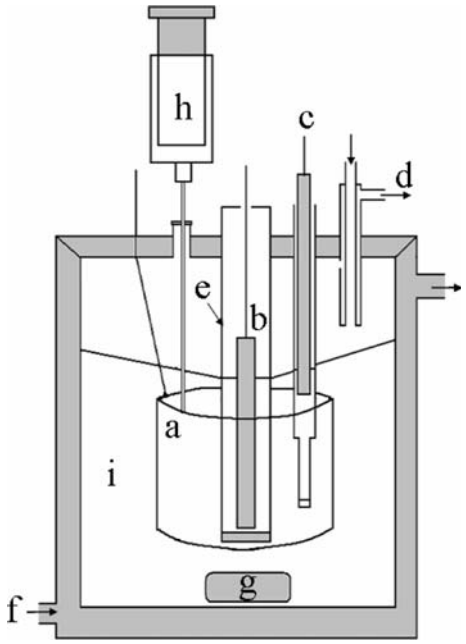

Fig. 2 Scheme of the electrolysis system for the reduction of UO_2^{2+} ions: a, Pt working electrode; b, Pt counter electrode; c, SCE reference electrode; d, Ar purge gas outlet; e, Vycor glass tube; f, coolant inlet; g, magnetic stirrer; h, sampling syringe; i, test solution

cell system was composed of a cylindrical Pt plate with a large surface area (32.7 cm^2) as a working electrode, a large mesh Pt counter electrode inserted into one closed-end porous Vycor glass tube and a saturated calomel electrode (SCE) with Luggin capillary as a reference electrode. A circulating water bath maintained the temperature of the test solution at 298 ± 0.5 K.

Potential control and current acquisition were conducted by a computerised potentiostat (EG&G PAR 273, USA). The concentrations of U^{4+} ions in a 1.0 M $HClO_4$ solution during the electrolysis were determined by measuring the UV/VIS (Milton Roy Spectronic 3000 array, USA) absorption intensity at 637 nm.

Three different kinds of working electrodes, which were made of platinum (Tacussel, France), gold (Tacussel) and static mercury drop (PARC, USA), were used to obtain the cyclic voltammograms of UO_2^{2+} ions. The exposed areas of platinum, gold and mercury electrodes amounted to 0.07, 0.07 and 0.015 cm^2, respectively.

3 Results and discussion

3.1 Role of Pt-OH_{ad} in the oxidation of dissolved hydrogen at a high temperature

Figure 3a illustrates the potentiodynamic polarisation curves obtained in deaerated and hydrogenated boric acid

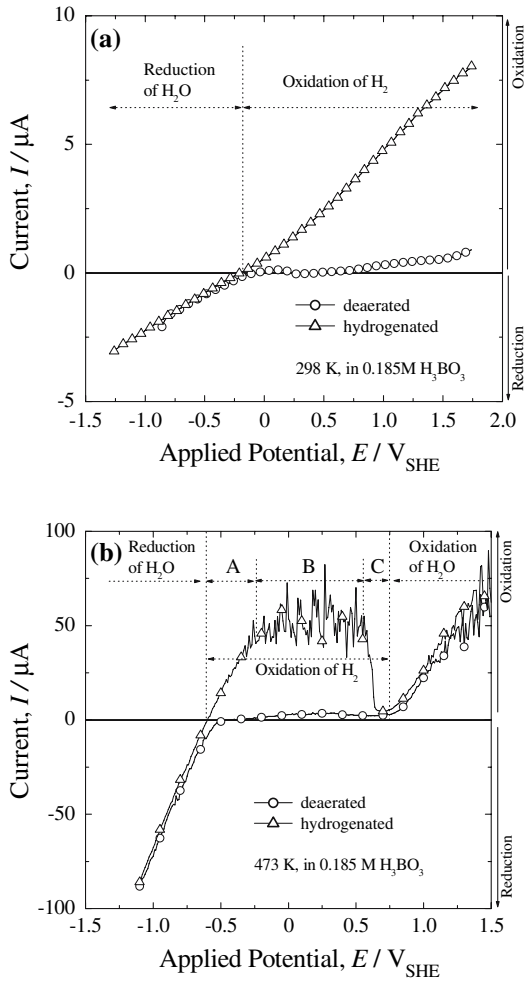

Fig. 3 Potentiodynamic polarisation curves at Pt electrode in a 0.185 M H_3BO_3 solutions conditioned with Ar(○) and H_2(△) at solution temperatures of (**a**) 298 K and (**b**) 473 K; scan rate, 5 mV s^{-1}; exposed electrode area, 0.03 cm^2

solutions on Pt electrode at room temperature. The applied potential was scanned from –1.25 to 1.75 V_{SHE} in the anodic direction at a scan rate of 5 mV s^{-1}. There was no particular electrochemical reaction except for the reduction and oxidation of water under deaerated condition. Under hydrogenated condition, the reduction current of water was observed to decrease as the applied potential increased from –1.25 to –0.20 V_{SHE}, while the oxidation current of dissolved hydrogen appeared to increase monotonically with increasing applied potential from –0.20 to 1.75 V_{SHE}.

It is well known [27] that the electrochemical oxidation of dissolved hydrogen at room temperature is controlled by electron transfer reaction (step 3), mass transfer reaction (step 1) and passivation reaction (steps 4 and 5) in sequence as the applied potential increases. However, in this polarisation curve, mass transfer limiting and passivation region were not observed due to a high ohmic potential drop caused by the low conductivity (8.9 μS cm^{-1}) of the electrolyte.

Figure 3b shows the potentiodynamic polarisation curves measured on Pt electrode in deaerated and hydrogenated boric acid solutions at 473 K. The applied potential was scanned from –1.10 to 1.50 V_{SHE} in the anodic direction at a scan rate of 5 mV s^{-1}. It should be noted that the value of the current measured at a high temperature was notably higher as compared with that value at room temperature in both conditions. Moreover, under deaerated condition, the polarisation curve was similar in shape to that curve measured at room temperature. In contrast, under hydrogenated condition, the polarisation curve was different in shape from that curve at room temperature. From the comparison between the current measured under deaerated and hydrogenated conditions, it was recognised that the reduction current measured in the applied potential range between –1.10 and –0.65 V_{SHE} is clearly attributable to the reduction of water, and the oxidation current in the potential range between –0.65 and 0.75 V_{SHE} is due to the oxidation of dissolved hydrogen. In addition, the oxidation current at the potentials higher than 0.75 V_{SHE} is ascribed to the oxidation of water.

The equilibrium potential at which the net current is zero was observed at the potential of –0.65 V_{SHE}. Compared with the equilibrium potential measured at room temperature shown in Fig. 3a, the equilibrium potential measured at 473 K shifted to more cathodic direction. This indicates that the increase of hydrogen oxidation current surpasses the increase of water reduction current at 473 K, thus the reducing capability of dissolved hydrogen increases at a high temperature.

The oxidation current of dissolved hydrogen can be divided into three different regions: the increase of the oxidation current in the potential range from –0.65 to –0.25 V_{SHE} in the first region (Region A), the potential-independent current plateau in the potential range from –0.25 to 0.60 V_{SHE} in the second region (Region B) and the steep decrease of the oxidation current with increasing applied potential from 0.60 to 0.75 V_{SHE} in the final region (Region C). The increase in the oxidation current in Region A means that the electron transfer reaction (step 3) is the rate-determining step.

The current plateau in Region B indicates that the oxidation of dissolved hydrogen is controlled by the mass transfer reaction, reaction 1. It is worthwhile noting that the behaviour controlled by the mass transfer reaction became dominant in Region B at a high temperature. The current oscillation on the plateau is ascribed to the adsorption and desorption of anions in the test solution [29, 30]. Finally, the steep decrease of the oxidation current in Region C corresponds to the preferential adsorption of hydroxyl radicals onto Pt surface to form Pt-OH_{ad} (or Pt-O), and thus

the hydrogen oxidation current became very small as a result of the decrease in the number of adsorption sites for the hydrogen atoms. This leads to passivation of Pt surface.

It is generally known that as temperature increases, both the mass transfer reaction (step 1) and electron transfer reaction regarding the homogeneous dissociation of molecular hydrogen and the desorption of hydrogen atoms from Pt surface (step 3) are enhanced. The enhancement of the mass transfer reaction is due to the increase of the mobility of dissolved hydrogen, and the enhancement of the electron transfer reaction is mainly ascribed to endothermic contribution [20, 31]. In addition, it is generally accepted that either Pt-OH_{ad} or Pt-O, which causes passivation of Pt, is further stabilised at a high temperature, while either Pt-OH_{ad} or Pt-O may be unstabilised in hydrogenated condition due to the high reduction power of dissolved hydrogen at a high temperature.

From the experimental result that the oxidation current plateau appeared in the potential range between –0.25 and 0.60 V_{SHE}, it was suggested that the increase of the mass transfer rate is overwhelmed by the increase of the electron transfer rate at 473 K in this potential range. Moreover, from the appearance of well-defined passivation region in the potential range between 0.60 and 0.75 V_{SHE}, it was recognised that either Pt-OH_{ad} or Pt-O is formed stably at 473 K to blockade the oxidation reaction of dissolved hydrogen.

3.2 Role of Pt-H_{ad} in the reduction of UO_2^{2+} ions in an acidic solution

It is known [14–18] that UO_2^{2+}ions are reduced to unstable UO_2^{+} ions first, and then UO_2^{+} ions are immediately disproportionated into U^{4+} and UO_2^{2+} ions in an acidic medium during the electrochemical reduction of UO_2^{2+} ions at Hg electrode. In order to investigate the electrochemical reduction of UO_2^{2+} ions at Pt electrode, cyclic voltammetric measurement was performed for UO_2^{2+}ions on Pt surface in a 1.0 M $HClO_4$ solution at a scan rate of 100 mV s^{-1}. The resulting cyclic voltammograms are shown in Fig. 4. They were measured during the scanning of the applied potential from 0.20 to –0.25 V_{SCE} in the cathodic direction.

In the absence of UO_2^{2+} ions (○), typical reduction of water into molecular hydrogen was observed at potentials lower than –0.18 V_{SCE}, and in the reverse scan oxidation wave corresponding to the oxidation of molecular hydrogen atoms emerged in the potential range of –0.23 to –0.15 V_{SCE}. On the other hand, in the presence of UO_2^{2+} ions (△), reduction wave of UO_2^{2+} ions was observed in the potential range between 0 and –0.21 V_{SCE} prior to the occurrence of hydrogen evolution below –0.21 V_{SCE}. In the reverse scan, UO_2^{2+} reduction current was also found in the potential range between 0 and –0.21 V_{SCE} after a trace of hydrogen

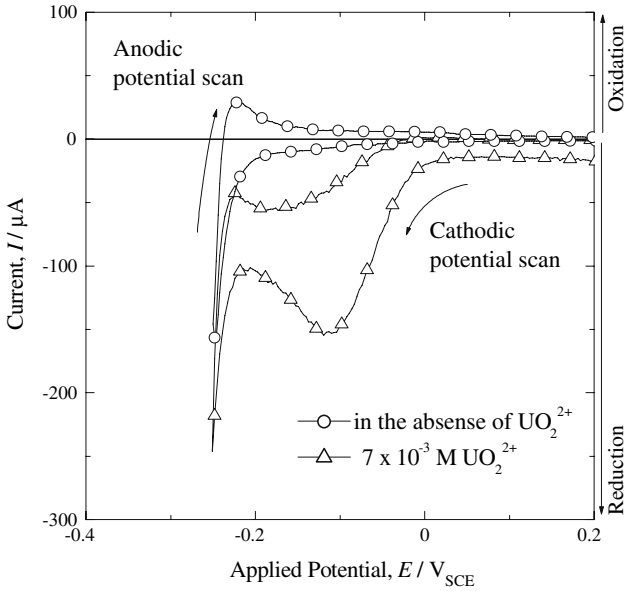

Fig. 4 Cyclic voltammograms for UO_2^{2+} ions at Pt electrode with a scan rate of 100 mV s^{-1} in a 1.0 M $HClO_4$ solution; UO_2^{2+} concentration, 0 M (○), 7 × 10^{-3} M (△); exposed electrode area, 0.07 cm^2

oxidation. Since the reduction waves of UO_2^{2+} ions appear in the hydrogen adsorption potential region between 0 and –0.21 V_{SCE} during both forward and reverse scans, it is plausible that Pt-H_{ad} may be involved in the reduction of UO_2^{2+} ions.

In order to elucidate the role of Pt-H_{ad} in the reduction reaction of UO_2^{2+} ions in more detail, the cyclic voltammograms were obtained from three different kinds of electrodes. Figure 5 shows the cyclic voltammograms measured on Pt(○), Au(□) and Hg(△) electrodes in a 1.0 M $HClO_4$ solution containing UO_2^{2+} ions at a scan rate of 100 mV s^{-1}. It is well known that hydrogen evolution takes place on Pt [32], Au [32] and Hg [15, 32] at potentials below –0.24, –0.26 and –1.0 V_{SCE}, respectively, in a 1.0 M acidic solution in the absence of UO_2^{2+} ions. Under these circumstances, it is reasonable to think that the reduction currents of Pt, Au and Hg electrodes, obtained at the potentials higher than the above, originate mainly from the reduction of UO_2^{2+} ions.

In Figure 5, the peak currents of UO_2^{2+} reduction waves on Pt, Au and Hg electrodes emerged at –0.11, –0.23 and –0.29 V_{SCE}, respectively. This indicates that the reduction region of UO_2^{2+} ions shifted to a lower potential region in the order Pt < Au < Hg. Considering that hydrogen overpotential in absolute value increases in the same order [20], the shift of the reduction region is clearly related to hydrogen overpotential of the electrode material. Accordingly, the experimental results shown in Fig. 5 indicate that the reduction reaction of UO_2^{2+} ions on Pt surface mainly

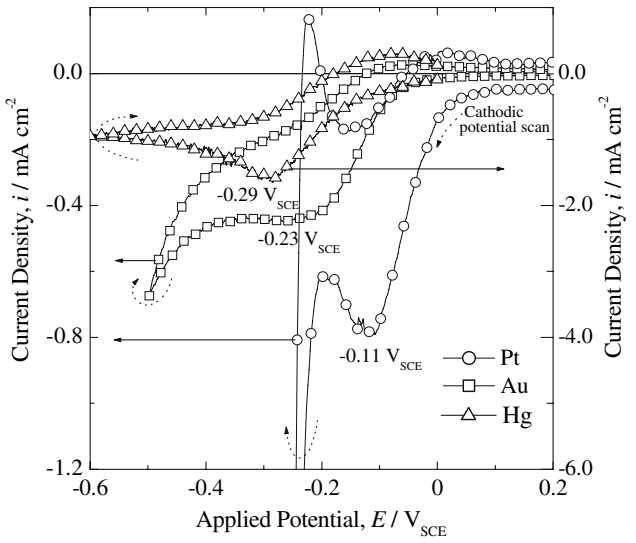

Fig. 5 Cyclic voltammograms for 4.3×10^{-3} M UO_2^{2+} at Pt (○), Au (□) and Hg (△) electrodes with a scan rate of 100 mV s^{-1} in a 1.0 M $HClO_4$ solution

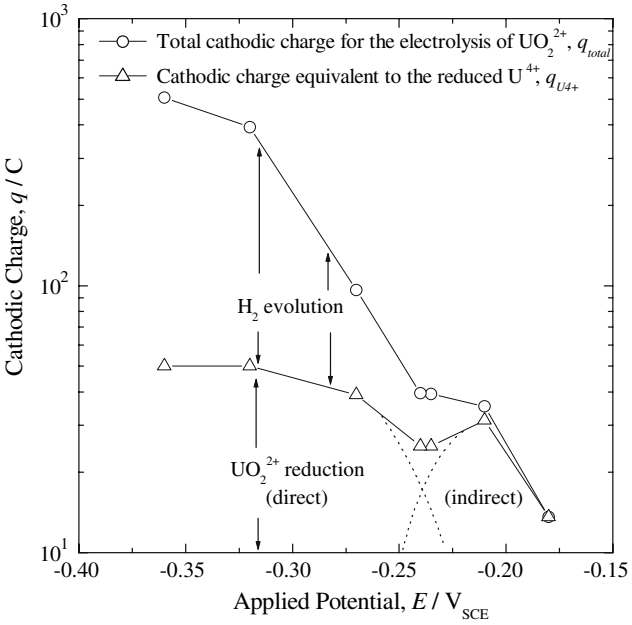

Fig. 6 Plots of the total cathodic charge for the electrolysis of UO_2^{2+} ions (○), q_{total}, and that cathodic charge equivalent to the reduced U^{4+} ions (△), q_{U4+}, against the applied potential E. Reduction of UO_2^{2+} ions was carried out by chronoamperometric method, and the reduced U^{4+} ions were determined by UV/VIS absorption spectrometric analysis; UO_2^{2+} concentration, 0.02 M; Pt electrode area, 32.7 cm^2; electrolyte, 1.0 M $HClO_4$; electrolysis time, 900 s

depends on the potential forming adsorbed hydrogen atoms on the electrode, rather than on the electrode potential ($UO_2^{2+} + e \rightarrow UO_2^{+}$: $E^o = 0.06$ V_{SHE} [16]). This result implies that there are two pathways for the reduction of UO_2^{2+} ions. One is a direct reduction of UO_2^{2+} ions ($UO_2^{2+} + e \rightarrow UO_2^{+}$), and the other is an indirect reduction of UO_2^{2+} ions by Pt-H_{ad}.

In the previous cyclic voltammograms as shown in Fig. 4, for UO_2^{2+} on Pt surface, UO_2^{2+} reduction was overlapped with that reduction of hydronium ions in the potential range below –0.18 V_{SCE}. In order to distinguish between these two reduction reactions more clearly, constant-potential electrolysis coupled with UV/VIS analysis was carried out. After each electrolysis test, the concentration of the reduced U^{4+} ions was estimated by measuring the UV/VIS absorption intensity.

The total cathodic charge needed for the electrolysis (○), q_{total}, and the cathodic charge equivalent to the concentration of the reduced U^{4+} ions (△), q_{U4+}, are plotted against the applied potential in Fig. 6. q_{total} increased exponentially as the applied potential decreased from –0.18 to –0.37 V_{SCE}. On the other hand, q_{U4+} increased as the applied potential decreased from –0.18 to –0.21 V_{SCE}, followed by the decrease of q_{U4+} in the potential range from –0.21 to –0.24 V_{SCE}, and then q_{U4+} increased again up to a constant value with decreasing applied potential from –0.24 to –0.37 V_{SCE}. It should be noted that q_{U4+} has a minimum value at the potential of –0.24 V_{SCE}.

From the fact that, in the potential range between –0.18 and –0.21 V_{SCE}, adsorbed hydrogen atoms are stable on Pt surface and the reduction reaction for UO_2^{2+} ions hardly occurs on Hg surface (shown in Fig. 5), it was recognised that the reduction charges obtained in this potential range are attributed to the indirect reduction of UO_2^{2+} ions by Pt-H_{ad}. In addition, it should be noted that the reduction of UO_2^{2+} ions to U^{4+} ions occurred with a very good current efficiency from the coincidence of q_{total} with q_{U4+} in this potential range.

However, it was found that the current efficiency became lower than ca. 100 % over the applied potential region below –0.21 V_{SCE}. Considering that there are no reducible species except UO_2^{2+} and hydronium ions in this potential range below –0.21 V_{SCE}, the difference between q_{total} and q_{U4+} is definitely attributed to the hydrogen evolution. This result indicates that Pt-H_{ad} contributes to the hydrogen evolution to some extent by the recombination reaction as well as to the reduction of UO_2^{2+} ions. As the applied potential decreases in the potential range from –0.21 to –0.24 V_{SCE}, the recombination reaction becomes more favourable, and then q_{U4+} corresponding to the reduction of UO_2^{2+} ions by H_{ad} decreases.

From the potential of –0.24 V_{SCE} on, q_{U4+} increases again with decreasing applied potential. Since there is no other factor causing the reduction of UO_2^{2+} ions except the electrochemical reduction by the electrons from the electrode in this potential region, the increase of the cathodic charge, q_{U4+}, obviously contributes to direct reduction of UO_2^{2+} ions. Moreover, from the fact that q_{U4+} approaches to

the constant value with decreasing applied potential below –0.32 V_{SCE}, it is considered that the reduction of UO_2^{2+} ions could be limited by the mass transfer reaction.

From the above results, it is recognised that the dominant reduction path of UO_2^{2+} ions is changed from indirect to direct reduction at the potential of –0.24 V_{SCE} as the applied potential decreases. This implies that the indirect reduction of UO_2^{2+} ions by Pt-H_{ad} is dominant in the potential range from –0.18 to –0.24 V_{SCE}, whereas the direct reduction of UO_2^{2+} ions by the electrons is dominant below –0.24 V_{SCE}. The potential of –0.24 V_{SCE} where q_{U4+} has a minimum value, is regarded as a transition potential of UO_2^{2+} reduction path from indirect to direct reduction.

On the basis of the experimental results and the well-known HER mechanism on Pt surface, an indirect reduction mechanism of UO_2^{2+} ions on Pt surface is proposed as follows:

$$Pt + H^+ + e \rightarrow Pt\text{-}H_{ad} \quad (6)$$

$$Pt\text{-}H_{ad} + UO_2^{2+} \rightarrow Pt\text{-}UO_2H_{ad}^{2+} \quad (7a)$$

$$Pt\text{-}UO_2H_{ad}^{2+} \rightarrow Pt + UO_2^{+} + H^+ \quad (7b)$$

$$UO_2^{+} + 2H^+ \rightarrow 1/2\ U^{4+} + 1/2\ UO_2^{2+} + H_2O \quad (8)$$

In indirect reduction, there are two possible paths for the reduction of UO_2^{2+} ions by H_{ad} atoms: One is the reaction of H_{ad} atoms with UO_2^{2+} ions adsorbed on Pt, and the other is the reaction of H_{ad} atoms with UO_2^{2+} ions in the solution. In the former case, the adsorption of UO_2^{2+} ions on Pt should take place prior to the reaction with H_{ad} atoms. Similar to catalyst poisons on hydrogen evolution, if the adsorbed UO_2^{2+} ions caused interference with the recombination step (H_{ad} + H_{ad} = H_2) of adsorbed hydrogen atoms, the hydrogen evolution potential might shift in the cathodic direction. However, on Pt surface, it was found that there was little change in the hydrogen evolution potential with the presence of UO_2^{2+} ions as shown in Fig. 4. For this reason, it is reasonable to consider that the latter path (steps 7a and 7b) is available for the reduction of UO_2^{2+} ions on Pt.

For the sake of clarity, the proposed reduction processes of UO_2^{2+} ions on Pt surface are schematically summarised in Fig. 7. The indirect reduction of UO_2^{2+} ions (steps 7a, 7b and 8) proceeds primarily by the reaction of UO_2^{2+} ions with Pt-H_{ad} in the potential range from 0 to –0.24 V_{SCE}, whereas the direct reduction of UO_2^{2+} ions (steps 9 and 10 [15–18]) proceeds in the potential range below –0.24 V_{SCE}.

$$UO_2^{2+} + e \rightarrow UO_2^{+} \quad (9)$$

$$UO_2^{+} + 2H^+ \rightarrow 1/2\ U^{4+} + 1/2\ UO_2^{2+} + H_2O \quad (10)$$

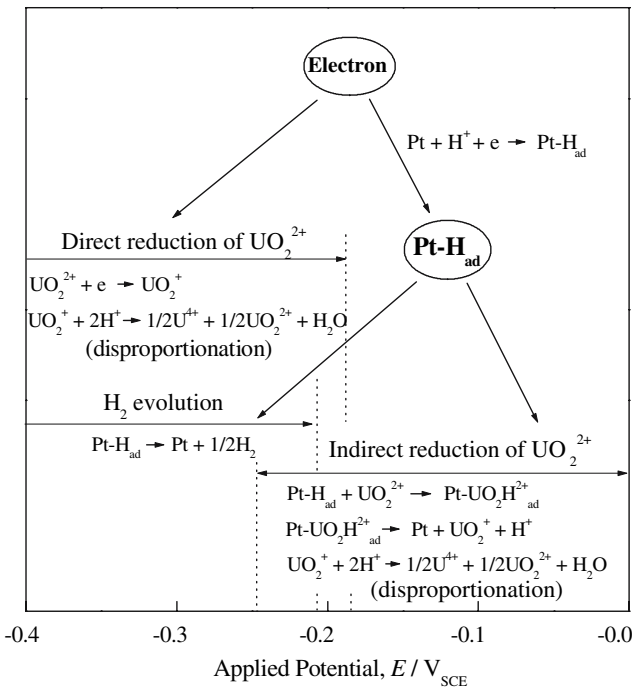

Fig. 7 Schematic diagram of proposed reduction mechanism of UO_2^{2+} ions on Pt electrode in an acidic solution

In addition, since hydrogen evolution occurs in a potential range lower than –0.21 V_{SCE}, a recombination reaction (step 11) of Pt-H_{ad} also takes place.

$$Pt\text{-}H_{ad} \rightarrow Pt + 1/2\ H_2 \quad (11)$$

4 Conclusions

From the analysis of the polarisation curves obtained from Pt electrode in a hydrogenated boric acid solution at 473 K, it is concluded that the hydrogen oxidation current is limited by the electron transfer, mass transfer and passivation reactions in sequence, as the applied potential increases. Especially, it is recognised that the passivation reaction is mainly attributed to a stable OH adsorption on Pt surface, Pt-OH_{ad}. From the analysis of the cyclic voltammograms determined from Pt electrode in a 1.0 M perchloric acid solution in the presence of uranyl ions, UO_2^{2+}, it is suggested that there are two pathways for the reduction of UO_2^{2+} to U^{4+} ions, implying that UO_2^{2+} ions can be reduced to U^{4+} ions not only by the electrons transferred from Pt electrode (direct reduction of UO_2^{2+}), but also by hydrogen atoms adsorbed on the electrode (indirect reduction of UO_2^{2+}). Moreover, from the comparison between total cathodic charge and cathodic charge equivalent to the concentration of U^{4+} ions during the constant-potential

electrolysis of UO_2^{2+} ions, the reduction mechanism of UO_2^{2+} ions on Pt surface is proposed and the transition potential from the indirect reduction to the direct reduction of UO_2^{2+} ions is determined.

Acknowledgments This work was supported by the Nuclear R&D Program of the Korean Ministry of Science and Technology (MOST). Incidentally, this work was partly supported by the Brain Korea 21 project. Furthermore, the authors are indebted to Mr. K.-N. Jung and Mr. K.-H. Na in CIERL at KAIST for their helpful comments.

References

1. Wood CJ (1995) PWR Primary Water Chemistry Guidelines: Revision 3, Report EPRI TR-105714. Electric Power Research Institute, Palo Alto, CA, USA
2. Ishigure K, Nukii T, Ono S (2006) J Nucl Mater 350:56
3. Fearnehough GD, Cowan A (1967) J Nucl Mater 22:137
4. Cowan A, Langford WJ (1969) J Nucl Mater 30:271
5. Smith E (1995) J Mater Sci 30:5910
6. Magnin T, Noël D, Rios R (1994) Mat Sci Eng A-Struct 177:L11
7. Symons DM (1999) J Nucl Mater 265:225
8. Burrill KA (1998) Some aspects of water chemistry in the CANDU primary coolant circuit, proceedings of JAIF Int. Conf. Water Chem. Nucl. Power Plants, Kashiwazaki, Japan, 13–16 October, p 426
9. Yeon J-W, Jung Y, Pyun S-I (2006) J Nucl Mater 354:163
10. Keller C (1971) The Chemistry of the Transuranium Elements. Verlag Chemie GmbH, Weinheim/Bergstr., Germany, p 77
11. Aramata A, Terui S, Taguchi S, Kawaguchi T, Shimazu K (1996) Electrochim Acta 41:761
12. Futamata M, Luo L, Nishihara C (2005) Surf Sci 590:196
13. Nowicka AM, Zabost E, Donten M, Mazerska Z, Stojek Z (2006) Bioelectrochemistry 71:126
14. Herasymenko P (1928) Trans Faraday Soc 24:272
15. Kolthoff IM, Harris WE (1946) J Am Chem Soc 68:1175
16. Kern DMH, Orlemann EF (1949) J Am Chem Soc 71:2102
17. Duke FR, Pinkerton RC (1951) J Am Chem Soc 73:2361
18. Linzbach G, Kreysa G (1988) Electrochim Acta 33:1343
19. Jung K-S, Sohn S, Ha Y, Eom T (1991) J Electroanal Chem 315:113
20. Bockris JO'M, Reddy AK (1973) Modern Electrochemistry, Plenum/Resetta ed. Plenum Press, New York, p 1141
21. Gileadi E, Kirowa-Eisner E, Penciner J (1975) Interfacial Electrochemistry. Addison-Wesley Publishing Company, London, p 293
22. Conway BE, Bai L (1986) J Electroanal Chem 198:149
23. Burk LD, O'Leary WA (1989) J Appl Electrochem 19:758
24. Gabe DR (1997) J Appl Electrochem 27:908
25. Marković NM, Grgur BN, Ross PN (1997) J Phys Chem B 101:5405
26. Conway BE, Tilak BV (2002) Electrochim Acta 47:3571
27. Varela H, Krischer K (2001) Catal Today 70:411
28. Macdonald DD, Scott AC, Wentrcek P (1979) J Electrochem Soc 126:1618
29. Horányi G, Visy Cs (1979) J Electroanal Chem 103:353
30. Krischer K, Lübke M, Eiswirth M, Wolf W, Hudson JL, Ertl G (1993) Physica D 62:123
31. Conway BE, Bockris JO'M (1957) J Chem Phys 26:532
32. Dean JA (ed) (1973) Lange's Handbook of Chemistry, 11th edn. McGraw-Hill, New York, p 6/17